Journal of Applied Mechanics and Technical Physics, Vol. 46, No. 3, pp. 307–314, 2005

DEVELOPMENT OF THE RICHTMYER–MESHKOV INSTABILITY UPON INTERACTION OF A DIFFUSION MIXING LAYER OF TWO GASES WITH SHOCK WAVES

G. A. Ruev,[1] A. V. Fedorov,[2] and V. M. Fomin[2]

UDC 532.517.4: 533.6.011.8

Based on the previously formulated mathematical model of mechanics of a two-velocity two-temperature mixture of gases, the evolution of an initially disturbed mixing layer of two gases with different densities under the action of shock waves is considered in a two-dimensional unsteady approximation. Problems of interaction of shock waves with a sinusoidally disturbed diffuse layer are solved numerically. The predicted variation of the mixing-region width are in satisfactory agreement with experimental data.

Key words: *shock wave, mixing layer, Richtmyer–Meshkov instability, two-velocity two-temperature gas dynamics of mixtures.*

Introduction. The mixing layer is traditionally considered as a discontinuity surface for density, i.e., as a contact discontinuity. Shock-wave interaction with a disturbed contact discontinuity generates the Richtmyer–Meshkov instability [1, 2]. The final stage of this process involves the formation of a turbulent mixing region separating the flows of compressed gases in the region of the initial contact discontinuity.

Numerous papers dealing with numerical simulations of the evolution of the Richtmyer–Meshkov instability (see, e.g., [3–5]) and based on the Euler equations did not take into account the influence of mutual penetration of the gases. In addition, it is known that substitution of a stepwise velocity profile on the contact discontinuity by a continuous distribution in a certain finite-width layer can ensure a lower growth rate of disturbances at the initial stage of development of the Richtmyer–Meshkov instability. This was noted, e.g., in [6, 7], where the disturbance-amplitude growth was considered theoretically, and in the experimental works [8–10]. Therefore, it seems of interest to study this problem on the basis of equations of a two-velocity two-temperature mixture of gases where each component of the mixture has its own velocity and temperature. This approach makes it possible to describe both the processes of mutual penetration of the gases and the interaction of the mixing layer with the shock wave. The necessity of using models of multispecies mixtures for the description of contact-boundary destruction and mixture formation was indicated in [11]. Youngs [5] constructed a semi-empirical model of turbulent mixing of a multispecies medium, based on the use of an individual velocity for each component. In this model, turbulent mixing is assumed to arise instantaneously. Processes that occur at the initial stages of the Richtmyer–Meshkov instability devlopment are considered below on the basis of equations of two-velocity two-temperature gas dynamics of mixtures.

Formulation of the Problem. We consider the evolution of a transitional layer separating two pure gases with different densities under the action of a shock wave within the framework of the model of a two-dimensional unsteady flow of a two-velocity two-temperature mixture. The problem formulation is illustrated in Fig. 1. A steady shock wave propagates from gas No. 2 to gas No. 1. The shock wave arrives at the boundary of the layer at the time $t = 0$. The shape of the centerline of the mixing layer is described by the equation $x_0(y) = a_0(1 - \cos(\theta y))$,

[1]Novosibirsk State University of Architecture and Civil Engineering, Novosibirsk 630008; ruev@sibstrin.ru. [2]Institute of Theoretical and Applied Mechanics, Siberian Division, Russian Academy of Sciences, Novosibirsk 630090; fedorov@itam.nsc.ru. Translated from Prikladnaya Mekhanika i Tekhnicheskaya Fizika, Vol. 46, No. 3, pp. 3–11, May–June, 2005. Original article submitted July 26, 2004.

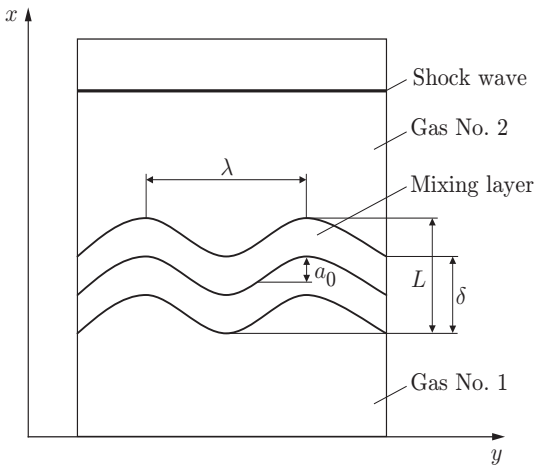

Fig. 1. Formulation of the problem.

where a_0 is the disturbance amplitude, $\theta = 2\pi/\lambda$ is the wavenumber, and λ is the disturbance wavelength. The total width of the mixing layer is denoted by L, and the initial diffusion width of the layer is denoted by δ.

The parameters of the mixture in the layer are described by the equations of two-velocity two-temperature gas dynamics of mixtures [12]:

$$\frac{\partial U_i}{\partial t} + \frac{\partial F_i^{(1)}}{\partial x} + \frac{\partial F_i^{(2)}}{\partial y} = W_i,$$

$$U_i = \begin{bmatrix} \rho_i \\ \rho_i u_i \\ \rho_i v_i \\ E_i \end{bmatrix}, \qquad F_i^{(1)} = \begin{bmatrix} \rho_i u_i \\ \rho_i u_i^2 + p_i \\ \rho_i u_i v_i \\ u_i E_i + p_i u_i \end{bmatrix}, \qquad F_i^{(2)} = \begin{bmatrix} \rho_i v_i \\ \rho_i v_i u_i \\ \rho_i v_i^2 + p_i \\ v_i E_i + p_i v_i \end{bmatrix},$$

$$W_i = \begin{bmatrix} 0 \\ K(u_j - u_i) \\ K(v_j - v_i) \\ Ku_i(u_j - u_i) + Kv_i(v_j - v_i) + \beta_i K((u_j - u_i)^2 + (v_j - v_i)^2) + q(T_j - T_i) \end{bmatrix}, \tag{1}$$

$$p_i = kn_iT_i, \quad E_i = \rho_i(e_i + (u_i^2 + v_i^2)/2), \quad e_i = kT_i/(\gamma_i - 1), \quad \rho_i = m_i n_i, \quad i, j = 1, 2 \ (i \neq j).$$

Here ρ_i is the density, u_i and v_i are the velocity components, e_i is the internal energy, p_i is the pressure, T_i is the temperature, m_i is the mass, n_i is the number density of a molecule of the ith kind, x and y are the Cartesian coordinates, t is the time, k is the Boltzmann constant, $K = 16\rho_1\rho_2\Omega_{12}^{(1,1)}/(3(m_1 + m_2))$, $\Omega_{12}^{(1,1)}$ is the collision integral, $\beta_i = m_iT_i/(m_1T_1 + m_2T_2)$, $q = 3m_1K/(m_1 + m_2)$, $c_{iv} = k/(m_i(\gamma_i - 1))$, and γ_i is the ratio of specific heats. The interaction potential for solid spheres is described by the relation

$$K = \frac{16}{3}\,\frac{\rho_1\rho_2}{m_1m_2}\sqrt{\frac{k\pi}{2}}\sqrt{\frac{T_1}{m_1} + \frac{T_2}{m_2}}\,\sigma_{12} \qquad \left(\sigma_{12} = \frac{\sigma_1 + \sigma_2}{2}\right),$$

where σ_i is the diameter of the molecule of the ith gas.

For low (or zero) concentrations of the jth gas, we use the Euler equations for the pure ith gas and determine the parameters of the other gas from the expressions

$$\frac{\partial n_j}{\partial t} + \frac{\partial n_j u_j}{\partial x} + \frac{\partial n_j v_j}{\partial y} = 0, \qquad u_j = u_i, \qquad v_j = v_i, \qquad T_j = T_i.$$

The transition to the heavy gas is performed if the molar concentration of the light gas is $x_j = n_j/(n_1 + n_2) < 1\%$, and the transition to the light gas is performed if the mass concentration of the heavy gas is $\alpha_j = \rho_j/(\rho_1 + \rho_2) < 1\%$.

Formation of the Initial Mixing Region. An asymptotic solution of the problem on formation of the initial diffusion layer in the one-dimensional approximation was obtained in [13]. Assuming that the distribution of parameters in each y section remains one-dimensional and that disturbances are present in the flow, we obtain the relation for the molar concentration from [13]

$$x_1 = \frac{1-\Phi(\eta)}{2} \qquad \Big(\Phi(\eta) = \frac{2}{\sqrt{\pi}} \int\limits_0^\eta \mathrm{e}^{-\omega^2}\, d\omega, \quad \eta = \frac{x - x_0(y)}{2\sqrt{Dt}}, \quad D = \frac{x_1 x_2 p}{K}\Big), \tag{2}$$

which satisfies the initial distribution of the molar concentration: $x_1 = 1$ for $x < x_0(y)$ and $x_1 = 0$ for $x > x_0(y)$.

Calculation Method. The flux vector splitting developed in [14] is used as a method for calculating the spatial approximation of system (1). To retain solution monotonicity in regions with high gradients, the order of approximation is reduced by a minmod limiter used for constructing TVD schemes [15]. We used the implicit approximation of the right sides of system (1) suggested in [12], which allowed us to avoid amplification of the constraint on the time step imposed by the Courant condition.

The computations were performed in a rectangular domain $[x_n, x_k; 0, \lambda/2]$. The conditions of zero derivatives were imposed on the lower and upper boundaries (x_n, x_k). To eliminate the influence of boundary conditions on the waves reaching these boundaries, the computational domain was extended. The side boundaries were subjected to conditions of symmetry.

The concentration distribution at the initial time is described by Eq. (2). The remaining parameters ahead of the shock-wave front have the following values: $u_i = v_i = 0$, $T_i = T_0 = 300$ K, $p = p_0 = 0.5$ atm, $n = n_0 = p_0/(kT_0)$, and $n_i = x_i n_0$. At the initial time, the shock wave is located in the x section (at the boundary of the layer) where the maximum concentration of gas No. 1 (molar concentration if gas No. 1 is light or mass concentration if gas No. 1 is heavy) equals 1%. The parameters behind the shock-wave front are determined by the Rankine–Hugoniot relations for gas No. 2.

Transition of the Shock Wave from the Light to the Heavy Gas. It is known that the shock-wave transition from the light to the heavy gas through a disturbed contact discontinuity is accompanied by formation of a refracted shock wave and a reflected shock wave. The shapes of these waves are similar to the shape of the disturbance of the initial contact boundary. A similar pattern is observed when the shock wave passes through a disturbed mixing layer. Nevertheless, the existence of a transitional region attenuates the growth of disturbances and adds some specific features to the Richtmyer–Meshkov instability evolution.

Figure 2 shows the isolines of the total pressure of the mixture at different times for a shock wave passing from argon to xenon (the numbers on the graphs indicate the values of the dimensionless pressure p/p_0). The dashed curves show the mixing-layer boundaries corresponding to the 1% molar concentration of argon and the 1% mass concentration of xenon. The computations were performed with the following values of parameters: $m_1/m_2 = 3.28$, $\sigma_2/\sigma_1 = 3.66/4.94$, Mach number M $= 3.5$, Atwood number A $= (\rho_h - \rho_l)/(\rho_h + \rho_l) = 0.53$, $\lambda = 36$ mm, $a_0 = 5$ mm, and $\delta = 10$ mm. For the monatomic gases under consideration, $\gamma_1 = \gamma_2 = 5/3$. When the shock wave passes from the light to the heavy has, the shape of the refracted shock wave is similar to the shape of the initial disturbance of the mixing layer. With distance from the mixing layer, the shock-wave front becomes straight. Reflected compression waves are simultaneously formed inside the mixing layer; the lift-up of these waves occurs outside the layer in gas No. 2. Interaction of the shock wave with the mixing layer results in compression of the layer and a simultaneous decrease in the disturbance amplitude. When the shock wave leaves the mixing layer, the disturbance amplitude starts growing, which is caused by elevated or reduced pressure values in regions where the shock wave is locally converging or locally diverging, respectively. As a result, there arises a heavy gas jet directed toward the light gas. Beginning from a certain moment (for the case considered, $t \approx 100$ μsec), a mushroom-shaped structure starts to form on the side boundaries of the jet, which is caused by generation of vortices with the centers inside the mixing layer, i.e., development of the Kelvin–Helmholtz instability begins.

Figure 3 shows the field of the mean-mass velocity of the mixture in a reference system moving with the velocity of the center of mass of the mixing layer. Origination of the vortex structure leads to intense growth of the mixing layer in the transverse direction and to deceleration of its growth in the streamwise direction. An increase in the layer width leads to interaction of the neighboring jets with each other and, subsequently, to emergence of a turbulent mixing region. The refracted and reflected shock waves become straight with time, and their parameters tend to the values obtained in [13] for a one-dimensional case.

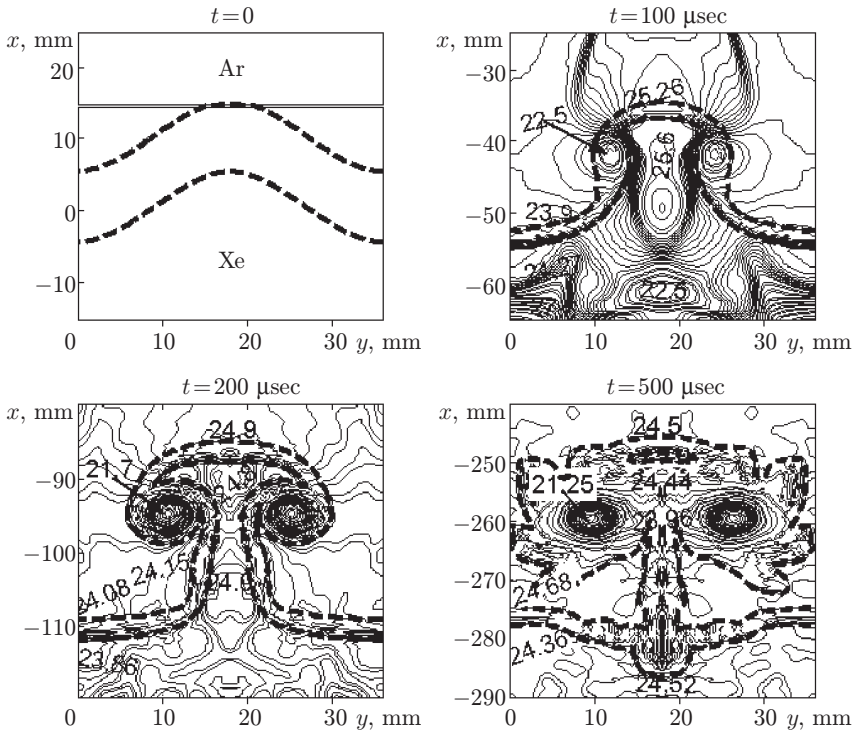

Fig. 2. Isolines of total pressure in the mixture at different times for the shock wave passing from argon to xenon.

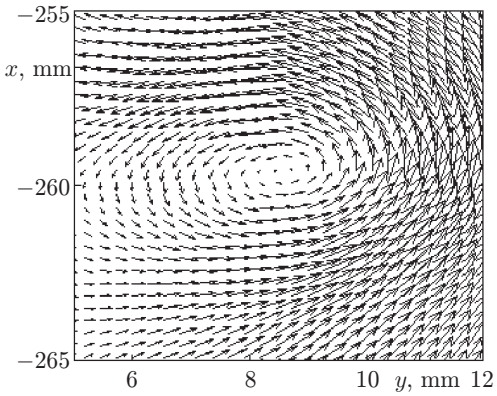

Fig. 3. Isolines of the mean-mass velocity of the mixture near the vortex center at $t = 500$ μsec.

Figure 4 shows the isolines of the molar concentration of the light gas for different values of the disturbance wavelength and the ratio of molecular weights (Atwood numbers) at the times $t = 50$ and 200 μsec after the beginning of shock wave–mixing layer interaction. We considered the shock-wave transition from argon to xenon and from helium to xenon ($m_1/m_2 = 32.8$, $\sigma_2/\sigma_1 = 2.19/4.94$, A = 0.82, and M = 3.5). It follows from Fig. 4 that a decrease in disturbance wavelength leads to an earlier formation of the mushroom-shaped structure on the jet surface and to a more intense expansion of the jet in the transverse direction, which induces interaction of the neighboring jets. Before origination of vortices, the mixing layer is rather thin and can be considered as a discontinuity surface. Yet, the development of the vortex structure leads to intense mixing and increases the layer width, which does not allow us to consider the mixing layer as a discontinuity surface any more. As the molecular weight increases, the depth of penetration of the heavy gas to the light gas also increases.

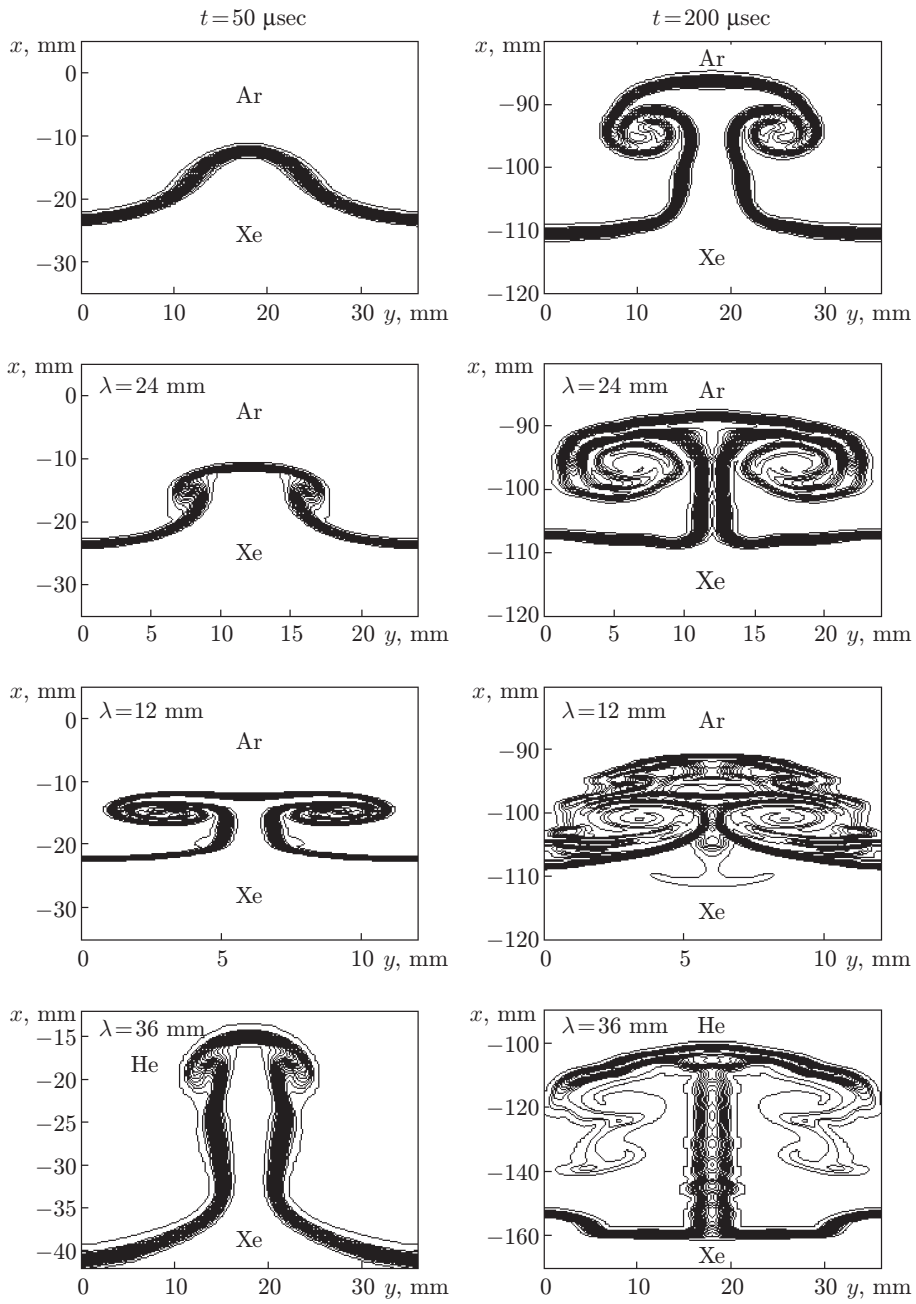

Fig. 4. Isolines of the molar concentration of the light gas for different values of A and λ at the times $t = 50$ and 200 μsec.

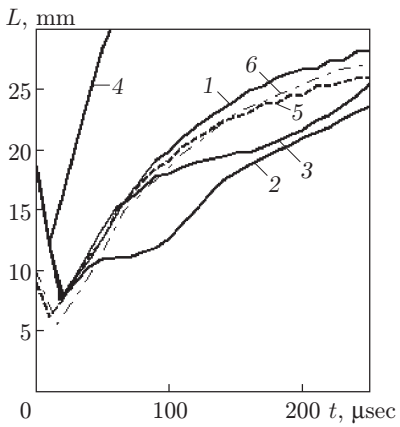

Fig. 5

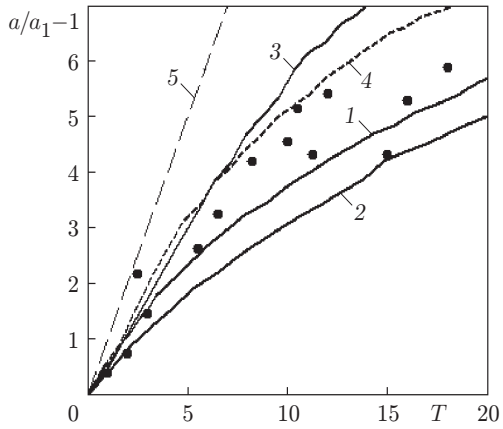

Fig. 6

Fig. 5. Time evolution of the total width of the mixing layer for different values of λ and δ_0, M = 3.5, and $a_0 = 5$ mm: curves 1–3 refer to the Ar → He transition, $\delta_0 = 10$ mm, and $\lambda = 36$ (1), 12 (2), and 24 mm (3); curve 4 refers to the He → Ar transition, $\lambda = 36$ mm, and $\delta_0 = 10$ mm; curve 5 refers to the Ar → Xe transition, $\lambda = 36$ mm, and $\delta_0 = 1$ mm; curve 6 shows the calculation results of [4].

Fig. 6. Time evolution of the disturbance amplitude for the shock wave (M = 2.5) passing from helium to argon for different values of λ, a_0, and δ_0: 1) $\lambda = 15$ mm, $a_0 = 1$ mm, and $\delta_0 = 8$ mm; 2) $\lambda = 15$ mm, $a_0 = 1$ mm, and $\delta_0 = 18$ mm; 3) $\lambda = 30$ mm, $a_0 = 1$ mm, and $\delta_0 = 8$ mm; 4) $\lambda = 30$ mm, $a_0 = 2$ mm, and $\delta_0 = 8$ mm; curve 5 shows the calculation by the Richtmyer formula; the points show the experimental results of [10].

Figure 5 shows the time evolution of the total width of the mixing layer for different values of disturbance wavelength and Atwood numbers. The shock wave passes from the light gas (argon or helium) to xenon. After compression of the mixing layer by the shock wave, at the linear stage of development of the Richtmyer–Meshkov instability, a smaller disturbance wavelength (curves 1 and 3) corresponds to a faster increase in the layer width. At the nonlinear stage, however, a decrease in λ leads to a lower growth rate of the mixing-layer thickness. This is caused by a more intense expansion of the layer in the transverse direction with decreasing wavelength. A typical feature for low values of λ (curve 2) is the absence of the linear stage, because the formation of the heavy gas jet and origination of vortices begin when the shock wave is still in the mixing layer. As the ratio of molecular weights increases, the time when the disturbance amplitude starts growing decreases and the growth rate of the layer width increases (curve 4). Figure 5 also shown the results (curve 5) calculated for a small initial diffusion width of the layer ($\delta_0 = 1$ mm), which are close to the calculation results based on the Euler equations (curve 6) obtained in [4] for an initially discontinuous density profile. Beginning from a certain time after shock-wave compression, the total width of the layer is weakly dependent on δ_0. Nevertheless, the total relative width of the layer L/L_0 decreases almost by a factor of 2 owing to a twofold increase in the initial value of δ_0.

The calculated growth rate of the disturbance amplitude for the shock-wave transition from helium to argon separated initially by the mixing layer is compared with the experimental data of [10] in Fig. 6. Here, $T = \mathrm{A}\,\theta u(t - t_1)$, a is the disturbance amplitude (distance between the points of the maximum and minimum depth of penetration of the heavy gas into the light gas), u is the mean velocity of the mixing layer, obtained in one-dimensional calculations, t_1 is the time when the shock wave leaves the layer, and a_1 is the value of a at $t = t_1$. The calculations were performed for M = 2.5. The calculation results are seen to agree with the corresponding experimental data. A decrease in the initial diffuse width of the layer leads to an increase in the disturbance-amplitude growth rate (curves 1 and 2). Similarly, the disturbance amplitude decreases with decreasing λ (curves 1 and 3). With increasing a_0, the disturbance amplitude growth faster at the initial stage of instability development, whereas its growth rate decreases at the nonlinear stage (curves 3 and 4). Figure 6 also shows the dependence $a/a_1 - 1 = \mathrm{A}\,ku(t - t_1)$ derived in [1] for an initially discontinuous density profile. Both in calculations and experiments, the disturbance-amplitude growth rate in the presence of the mixing layer is smaller than that at the interface with a discontinuous change in density.

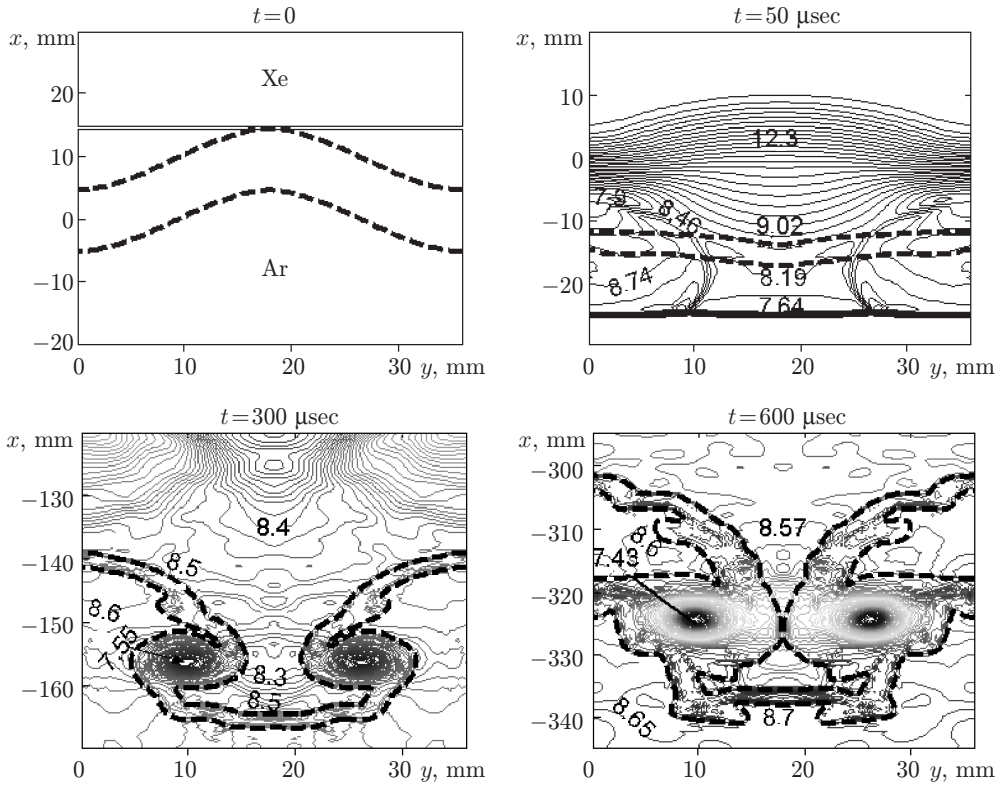

Fig. 7. Isolines of the total pressure of the mixture at different times for the shock wave passing from xenon to argon.

Transition of the Shock Wave from the Heavy to the Light Gas. Figure 7 shows the evolution of the mixing layer and the total pressure isolines for the shock wave passing from xenon (heavy gas) to argon ($M = 3.5$, $\lambda = 36$ mm, and $\delta = 10$ mm). The dashed curves indicate the mixing-layer boundaries. The numbers on the graphs are the values of the dimensionless pressure p/p_0. The shape of the refracted shock wave is convex toward the light gas, i. e., it is in antiphase to the initial shape of the layer boundary. Rarefaction waves propagate toward the heavy gas. First, the mixing layer becomes straight, and then a change in the disturbance phase occurs. After that, a heavy gas jet appears with subsequent formation of the mushroom-shaped structure and formation of vortices at the jet boundary with the center in the mixing layer, similar to that observed in the case of shock-wave transition from the light to the heavy gas.

Figure 8 shows the dependence $L(t)$ for different disturbance wavelengths (curves 1–3). At the initial stage of instability development, a smaller disturbance wavelength corresponds to a faster increase in the layer width. In the course of time, a decrease in the disturbance wavelength leads to earlier origination of vortex structures and to intense growth of the mixing layer in the transverse direction and a decrease in the layer width in the streamwise direction (e.g., curves 1 and 3). For $M = 3.5$, an increase in the ratio of molecular weights (curve 4) leads to deeper penetration of the heavy gas (Xe) jet to the light gas (He).

Conclusions. The mathematical model of the two-velocity two-temperature mixture of gases [12, 13] is applied in the present work to describe processes that occur upon interaction of shock waves with a sinusoidally disturbed region of mixing of two gases.

The wave patterns arising in the flow with the shock wave passing from the light to the heavy gas and from the heavy to the light gas are analyzed. Allowance for the initial finite width of the mixing layer decreases the growth rate of the normalized width of the layer.

It is found that vortices with the centers in the mixing layer are formed on the jet boundaries; each component in these vortices is characterized by its own velocity. Origination of such vortex structures leads to intense expansion of the layer in the transverse direction, which, in turn, leads to interaction of the neighboring jets.

The mathematical model is verified by the measured growth rates of the mixing-layer disturbance amplitude.

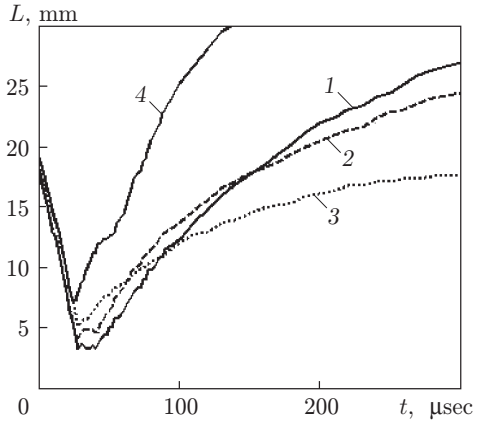

Fig. 8. Time evolution of the total width of the mixing layer for different values of λ and M = 3.5: curves 1–3 refer to the Xe → Ar transition and $\lambda = 36$ (1), 24 (2), and 12 mm (3); curve 4 refers to the Xe → He transition and $\lambda = 36$ mm.

This work was partly supported by the Russian Foundation for Basic Research (Grant No. 03-01-00453) and by the Ministry of Education of the Russian Federation (project of the long-term plan of the Novosibirsk State University of Architecture and Civil Engineering, dated March 1, 2003).

REFERENCES

1. R. D. Richtmyer, "Taylor instability in shock acceleration of compressible fluids," *Communs Pure Appl. Math.*, **13**, 297–319 (1960).
2. E. E. Meshkov, "Instability on a shock-wave accelerated interface of two gases," *Izv. Akad. Nauk SSSR, Mekh. Zhidk. Gaza*, No. 5, 151–157 (1969).
3. O. M. Belotserkovskii, V. V. Demchenko, and A. M. Oparin, "Consecutive transition to turbulence in the Richtmyer–Meshkov instability," *Dokl. Ross. Akad. Nauk*, **334**, No. 5, 581–583 (1994).
4. I. G. Lebo, V. V. Nikishin, V. B. Rozanov, and V. F. Tishkin, "On the effect of boundary conditions on the instability growth at a contact surface in passage of a shock wave," *Bull. Lebedev Phys. Inst.*, No. 1, 40–47 (1997).
5. D. L. Youngs, "Numerical simulation of mixing by Rayleigh–Taylor and Richtmyer–Meshkov instabilities," *Laser Particle Beams*, **12**, No. 4, 725–750 (1994).
6. S. Chandrasekhar, *Hydrodynamics and Hydromagnetic Stability*, Oxford Univ., Oxford (1961), pp. 428–436.
7. B. B. Chakraborty, "Rayleigh–Taylor instability of heavy fluid," *Phys. Fluids*, **18**, No. 8, 1066, 1067 (1975).
8. R. E. Duff, F. H. Harlow, and C. W. Hirt, "Effects of diffusion on interface instability between gases," *Phys. Fluids*, **5**, No. 4, 417–425 (1962).
9. M. Brouillette and B. Sturtevant, "Experiments on the Richtmyer–Meshkov instability: Single-scale perturbations on a continuous interface," *J. Fluid Mech.*, **263**, 271–292 (1994).
10. S. G. Zaitsev, S. N. Titov, and E. I. Chebotareva, "Evolution of the transitional layer separating gases of different densities with a shock wave passing through the layer," *Izv. Ross. Akad. Nauk, Mekh. Zhidk. Gaza*, No. 2, 18–26 (1994).
11. V. F. Kuropatenko, "Unsteady flow of multispecies media," in: *Numerical Methods of Solving Filtration Problems. Dynamics of Multiphase Media* (collected scientific papers) [in Russian], Inst. Theor. Appl. Mech., Sib. Div., Acad. of Sci. of the USSR (1989), pp. 128–155.
12. S. P. Kiselev, G. A. Ruev, A. P. Trunev, et al., *Shock-Wave Processes in Two-Component and Two-Phase Media* [in Russian], Nauka, Novosibirsk (1992).
13. G. A. Ruev, A. V. Fedorov, and V. M. Fomin, "Evolution of the diffusion mixing layer of two gases upon interaction with shock waves," *J. Appl. Mech. Tech. Phys.*, **45**, No. 3, 328–334 (2004).
14. W. K. Anderson, J. L. Thomas, and B. van Leer, "Comparison of finite volume flux vector splittings for the Euler equations," *AIAA J.*, **24**, No. 9, 1453–1460 (1986).
15. S. R. Chakravarthy and S. Osher, "A new class of high accuracy TVD schemes for hyperbolic conservation laws," AIAA Paper No. 85–0363 (1985).